FFEMS Fatigue & Fracture of Engineering Materials & Structures
ORIGINAL CONTRIBUTION
doi: 10.1111/ffe.12364

A relative crack opening time correlation for corrosion fatigue crack growth in offshore structures

O. ADEDIPE, F. BRENNAN and A. KOLIOS

Cranfield University, Bedfordshire MK43 0AL, United Kingdom

Received Date: 18 June 2015; Accepted Date: 20 September 2015; Published Online: 21 October 2015

ABSTRACT A considerable amount of research has been carried out on the prediction of mean stress effects on fatigue crack growth in structures. Newer types of structure are now being developed for use in highly dynamic, harsh marine environments, particularly for renewable energy applications. Therefore, the extent to which mean stresses can enhance corrosion-assisted fatigue damage in these structures needs to be better understood. A new theoretical model that accounts for mean stress effects on corrosion fatigue crack growth is proposed. The model is developed based on the relative crack opening period per fatigue cycle and by considering only the damaging portion of the stress cycle. The baseline data for the modelling exercise are the data obtained at a stress ratio of 0.1 in air and seawater tests conducted on compact tension specimens. The model is validated by comparison with experimental data and with other fatigue crack propagation models. The proposed model correlates fairly well with experimental data and the other models examined.

Keywords corrosion fatigue; crack growth rate; crack opening; mean stress; stress intensity factor.

NOMENCLATURE

A	= amplitude
a_1	= area of crack opening segment corresponding to positive R-ratio
a_2	= area of crack opening segment at a negative R-ratio
C	= coefficient in crack growth relationship
C_{air}	= coefficient in crack growth relationship in air
C_{corr}	= coefficient in crack growth relationship in seawater
C_0	= coefficient in crack growth relationship at an R-ratio of 0
$\frac{da}{dN}$	= crack growth rate
$\frac{da}{dN}_{air\ R=-1}$	= crack growth rate in air at an R-ratio of −1
$\frac{da}{dN}_{corr(R=-1)}$	= crack growth rate in seawater at an R-ratio of −1
$\frac{da}{dN}_{corr(+veR)}$	= crack growth rate in seawater at positive R-ratios
exp	= exponential
$K_{\max}$	= maximum stress intensity factor
K_{op}	= stress intensity factor at crack opening stress
M	= correction factor in Huang and Moan's model
m	= exponent in crack growth relationship
m_{air}	= exponent in crack growth relationship in air
m_{corr}	= exponent in crack growth relationship in seawater
m_0	= exponent corresponding to an R-ratio of 0
$P_{\max}$	= maximum applied load in a cycle
$P_{\min}$	= minimum applied load in a cycle
R	= stress ratio or R-ratio
sin	= sine of a function
ω	= angular velocity
ΔK	= stress intensity factor range

Correspondence: O. Adedipe. o.adedipe@cranfield.ac.uk, adelordy2002@yahoo.com

ΔK_{eff} = effective stress intensity factor range
ΔK^{+} = positive part of applied stress intensity factor range
ΔK^{*} = effective crack driving force parameter
$\sigma_{\min}$ = minimum applied stress in a cycle
$\sigma_{\max}$ = maximum applied stress in a cycle
γ = Walker's exponent
$\varnothing$ = correction factor in the model of Zhan *et al.*
π = pi
β = parameter in Huang and Moan's model
β_1 = parameter in Huang and Moan's model
α = constant in Kujawski's model

INTRODUCTION

Fatigue cracks in components and structures are undesirable and could propagate to failure or collapse when the load carrying capacity of the structural member is unable to withstand the externally applied cyclic loads. Cracks or defects can be introduced into structural members during fabrication, transportation or installation. Mean stresses may also be introduced into structural members during fabrication due to residual stresses. Offshore support structures are fabricated from rolled steel through longitudinal and circumferential welding processes. These structures experience significant levels both of cyclic loads and the harsh marine environment during service. Corrosion can amplify fatigue crack growth in the structures depending on the magnitude of the loads and the degree of stress concentration induced by existing defects. Therefore, to avoid economic losses, it is necessary to employ suitable monitoring tools that can detect fatigue cracks and the extent of the damage so that reliable life predictions can be made. The accuracy of such predictions is important for cost effective and optimal design of offshore structures.

Corrosion fatigue is a complex phenomenon due to the nature of the electrochemical interaction of material and the corrosive environment. The corrosion damage process is time dependent, and the frequency content of the applied stress cycle is an important variable.[1] At a lower loading frequency, more time is spent in exposing the crack tip to the corrosion effects and this accelerates the crack growth rates. In previous studies, the effect of loading frequency on crack growth rates in seawater was reported to be more damaging at lower cyclic load frequency. For example, in the work of Thorpe *et al.*,[2] it was found that crack growth rates in BS4360 50D steel in seawater were significantly enhanced at a lower frequency, but at a higher frequency, crack growth rates were found to be similar to those measured in an air environment. A similar phenomenon was also reported by Vosikovsky for X65 pipeline steel tested in 3.5% salt water.[3] A higher load frequency was also reported to have negligible effects on crack growth rates in 12Ni-5Cr-3Mo maraging steel tested in 3% sodium chloride solution.[4] In high-strength aluminium alloy, Gingell and King[5] reported that an increase in loading frequency led to reduction in crack growth rates in salt water, while in air, crack growth rates were found to be independent of loading frequency. More recently, the damaging effect of seawater was also reported by Adedipe *et al.*,[6] as crack growth rates in S355J2 + N steel were found to be higher than those measured in air across all the stress intensity factor ranges tested. The studies reported previously suggest that the environmental influence of seawater on crack growth rates is more dominant at lower frequencies than at higher ones. In an air environment, the effect of loading frequency has been reported to be negligible.[3,7] However, corrosion fatigue is not only frequency dependent but the process is also driven by a number of variables that cannot be studied by a single model. This is because each variable plays an important role in the corrosion fatigue process, making it a challenging and costly task to study experimentally. The interaction of a particular variable such as R-ratio with the environmental test condition may also have some influence on crack growth rates. For example, in 2 and 8, at more negative cathodic potentials, crack growth rates were significantly influenced at higher R-ratios compared with those obtained under a free corrosion potential. At an R-ratio of 0, in an aerated 3.5% sodium chloride solution, Kermani and Harrop[9] also found that crack growth in BS4360 50D steel increased at a more negative potential than at free corrosion potential. Some previous studies have also examined the effects of loading waveform on crack growth rates. In the work of Thorpe *et al.*,[2] crack growth rates in BS4360 50D steel in seawater using triangular waveform were found to be slightly lower than those measured using sinusoidal waveforms. However, they concluded that the crack growth rates obtained using sinusoidal waveforms were generally in agreement with those measured using triangular, positive and negative sawtooth waveforms. Appleton[10] also observed that, under a free corrosion condition, crack growth rates in

C-Mn steel tested using both triangular and sinusoidal waveforms were similar. In Barsom's work,[11] no effects of waveform on crack growth rates in 12Ni-5Cr-3Mo maraging steel was evident in an air environment, but under a sinusoidal waveform, for tests conducted in salt water, crack growth rates were significantly influenced at loading frequencies of 0.1, 1 and 10 Hz, respectively. Barsom also found that the crack growth rates obtained using a positive sawtooth waveform were approximately three times faster than those measured under a negative sawtooth waveform. The latter results were explained in terms of the shorter time available for a marked effect of salt water on crack growth at the loading portion of the stress cycle. This implies that corrosion-assisted crack growth depends on the available time that the crack tip is exposed to the corrosive environment during the loading portion of the stress cycle. However, the effect of waveform is not within the scope of this paper as the results discussed in the later sections are primarily based on mean stress or R-ratio effects on crack growth rates measured using sinusoidal waveforms. The degree to which corrosion fatigue crack growth can occur in offshore support structures also depends on various load interactions that are either applied locally or induced by residual stress at different parts of the structures with the likelihood of different behaviours at the weld areas. Residual stresses can influence the mean or maximum value of applied stress cycle and hence fatigue damage.[12] This implies that the stress level plays a significant role in the corrosion fatigue mechanism. Therefore, such load interaction effects may pose significant levels of mean stresses during service and may be accounted for in fatigue analysis using crack propagation models. It was also mentioned that mean stresses can significantly influence crack growth rates and must therefore be introduced in crack growth prediction models.[13]

Therefore, the extent to which mean stresses can enhance damage in offshore structures needs to be better understood so that appropriate material data for predicting the lifetime to be expected of structures in service can be determined. In this paper, a theoretical model to study the effects of stress ratio on fatigue crack growth in air and seawater is proposed, based on the relative opening area of the damaging portion of a fatigue cycle. The most widely used method for predicting fatigue crack growth is the Linear Elastic Fracture Mechanics concept, which was first introduced by Paris and Erdogan[14] as a relationship between crack growth rates and cyclic stress intensity factor ranges ΔK. The stress intensity factor is a variable that characterises the stress field in the vicinity of the crack. The stress intensity factor (ΔK) is recognised as the crack driving parameter as a fatigue crack extends through the thickness of the material at a corresponding crack growth rate. The Paris equation is expressed as

$$\frac{da}{dN} = C(\Delta K)^m, \tag{1}$$

where $\frac{da}{dN}$ is the crack growth rate, ΔK is the stress intensity factor range, C and m are material constants that depend on loading conditions and the environment. The controlling parameter in crack growth prediction is the crack length and/or depth. This implies that the remaining life of a structural member can be determined by integrating Eq. (1) from the initial crack length to the final crack length.

Mean stress effects are associated with stress ratio or R-ratio that can be expressed as a ratio of applied minimum stress to applied maximum stress in a fatigue cycle.

$$R = \frac{\sigma_{\min}}{\sigma_{\max}} \tag{2}$$

Mean stress effects can be schematically represented by Fig. 1 for a particular material under increasing or reducing R-ratio. Several models have been proposed to account for mean stress effects on fatigue crack growth, as modifications to the Paris law, because of its limitation to account for R-ratios effects. Such models are capable of representing fatigue crack growth data with different curve fitting parameters. Some of these models are discussed in the next section of this paper.

MEAN STRESS MODELS

A fatigue crack closure concept was introduced by Elber,[16] expressing crack growth rate as a function of the effective stress intensity factor range ΔK_{eff}, such that

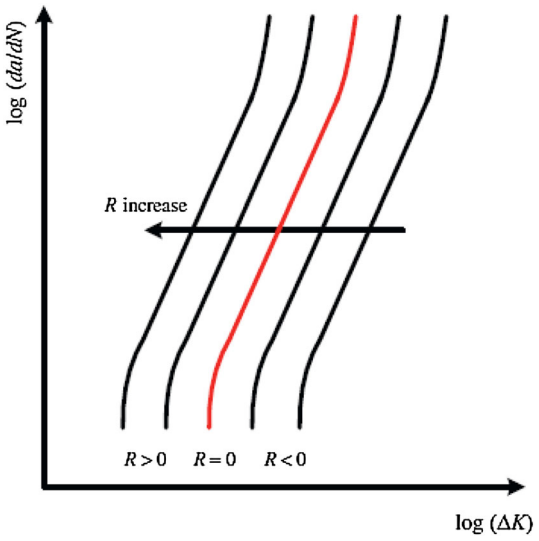

Fig. 1 R-ratio effect on fatigue crack growth.[15]

Eq. (1) is modified to be

$$\frac{da}{dN} = C(\Delta K_{\text{eff}})^m \tag{3}$$

$$\Delta K_{\text{eff}} = K_{\max} - K_{\text{op}}, \tag{4}$$

where K_{op} is the corresponding stress intensity factor at the crack opening stress. Various effective stress intensity factor correlations have also been introduced,[17–19] and also plasticity-induced crack closure models.[13,20] However, studies suggest that the crack closure concept was overestimated in the past, coupled with the difficulty in obtaining appropriate K_{op} during experimental tests.[21–23]

Walker[24] introduced an empirical relationship that incorporates mean stress effects. A third curve fitting parameter was also introduced to the Walker model, which adjusts the stress intensity factor (ΔK) to produce similar crack growth as $K_{\max}$ at R-ratio of 0. Walker's model can be expressed as

$$\frac{da}{dN} = C\left(\frac{\Delta K}{(1-R)^{(1-\gamma)}}\right)^m, \tag{5}$$

where γ is the Walker's exponent. Walker's model is only limited to positive R-ratio and was later modified by Kujawski[25] to account for mean stress at negative R-ratio. Kujawski introduced a two-parameter driving force for fatigue crack growth of aluminium alloys. The model is expressed as

$$\Delta K^* = \left(K_{\max}\Delta K^+\right)^{0.5} \tag{6}$$

Equation (6) was developed on the premise of predicting the mean stress effect without using the crack closure concept and based on the fact that for negative R-ratio, the compressing part of the fatigue cycle does not contribute to crack growth. Equation (6) was later modified[26] as

$$\Delta K^* = (K_{\max})^{\alpha}\left(\Delta K^+\right)^{1-\alpha}, \tag{7}$$

where ΔK^+ is the positive or damaging part of the stress intensity factor range, while α is an empirical curve fitting parameter. It has been stated that Eq. (7) yields a good correlation for most aluminium alloys and some other metallic materials.[25–27] However, it has also been mentioned that the model was better for correlating data at positive R-ratios compared with negative values.[28,29]

Huang and Moan[29] introduced an improved crack growth model that is capable of collapsing all crack growth curves to that corresponding to an R-ratio of 0. This implies that Eqs (8) and (9) can be used to predict crack growth rate at an R-ratio of interest using the material constants derived at an R-ratio of 0.

$$\frac{da}{dN} = C_0(M\Delta K)^{m_0}, \tag{8}$$

where C_0 and m_0 are the determined material constants at R-Ratio of 0.

$$M = \begin{cases} (1-R)^{-\beta_1} & -5 \le R < 0 \\ (1-R)^{-\beta} & 0 \le R < 0.5 \\ \left(1.05 - 1.4R + 0.6R^2\right)^{-\beta}, & 0.5 \le R < 1 \end{cases}, \tag{9}$$

where $\beta_1 = 1.2\beta$, β, β_1 are parameters, but how they were derived was not described in Huang and Moan's paper.[29] However, they did mention that the stated values of the parameters were just for illustration purposes only, as more investigation would be needed to determine them absolutely.

An approximate model similar to that developed by Huang and Moan was also proposed by Zhan *et al.*[15] to account for the effect of stress ratios on fatigue crack growth. The model was developed using aluminium alloys and medium carbon steel data taken from the literature at various stress ratios. The model is valid for stress ratios in the range $-1 \le R \le 1$ and can be used to predict crack growth rate at various stress ratios when only the data at $R = 0$ are obtained experimentally. The model is expressed as

$$\frac{da}{dN} = C_0(\varnothing\Delta K)^{m_0}, \tag{10}$$

where $\varnothing$ is a correction factor that depends on the R-ratio. The material response data in Eq. (10) are the same as those given by Huang and Moan in Eq. (8). The correction factor can be defined as

$$\varnothing = \exp(\alpha R) \tag{11}$$

From an extensive analysis using experimental data taken from the literature, the value of $\alpha = 0.65$ was assigned to low strength metallic materials, $\alpha = 0.75$ for high-strength metallic materials, such as Ti- alloys, while a value of $\alpha = 0.65$ was set for all other metallic materials.

A NEW MODEL TO ACCOUNT FOR THE STRESS RATIO EFFECT ON CORROSION FATIGUE CRACK GROWTH

A new theoretical model based on the relative crack opening period area ratio is proposed for predicting the corrosion fatigue crack growth rate at different stress ratios, depending on the two fatigue crack growth driving parameters ΔK and $K_{\max}$. The model is valid for stress ratios in the range $-1 \le R \le 0.9$ and is proposed using the

constant amplitude loading material response data derived at an R-ratio of 0.1 in air and seawater as the baseline. The major assumption of the correlation is that corrosion fatigue damage is equivalent to the proportion of time that the fatigue crack is open over a range of loading cycles. This is based on the rationale that the compressive portion of the loading cycle does not contribute to corrosion fatigue damage, that is, only half the time of the loading cycle is spent in the damaging or crack opening situation for a fully reversed cycle.

The physical basis for the model development is shown in Fig. 2. The figure describes the increasing and reducing R-ratio cases coupled with the representation of tensile and compressive portions of loading cycles at an R-ratio of −1. It is assumed in this work that the area of the damaging part of the fully reversed loading is related to the area under the applied stress cycle at an R-ratio of 0.1. As the mean stress or R-ratio is increased, for example, from 0.1 to 0.2, the applied stress cycle shifts above the corresponding stress cycle of an R-ratio of 0.1, as shown in the figure. The degree of shift above the R-ratio of the 0.1 stress cycle is a function of the level of the imposed mean stress or R-ratio. The hypothesis here is that the area under the applied stress cycle of a specific positive R-ratio, with reference to an R-ratio of 0.1, can be used as a correction to obtain the crack growth rates corresponding to that particular R-ratio. A description of the areas under the sine curve corresponding to the applied stress cycles at R-ratios of 0.2 and −1 with respect to an R-ratio of 0.1 is shown in Fig. 3.

Ideally, in an air environment, the fatigue crack closure occurs when the crack is under a compressive stress field and opens when a tensile stress field is applied. This effect results in some changes in the externally applied load and subsequent changes in the applied stress intensity factor range. Therefore, the effects of the residual stresses, which can also be described as crack opening and closing situations, can also be accounted for in crack growth rates by considering the residual stresses as mean stresses. This concept is employed in this study. The methodology for the model development that considers positive and negative stress ratios is described in the next section of the paper.

Positive R-ratios

For positive R-ratios, the model is schematically shown in Fig. 4 for a constant amplitude loading case. The left and right sides of the figure are equivalent to each other

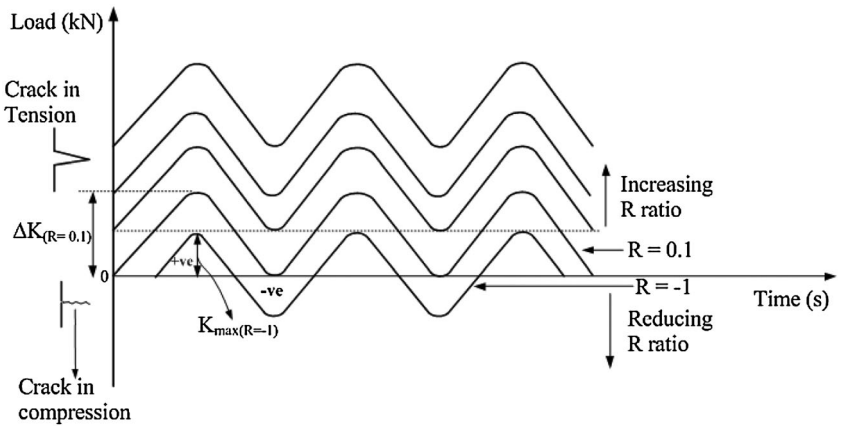

Fig. 2 Superimposed stress patterns for positive and negative R-ratios.

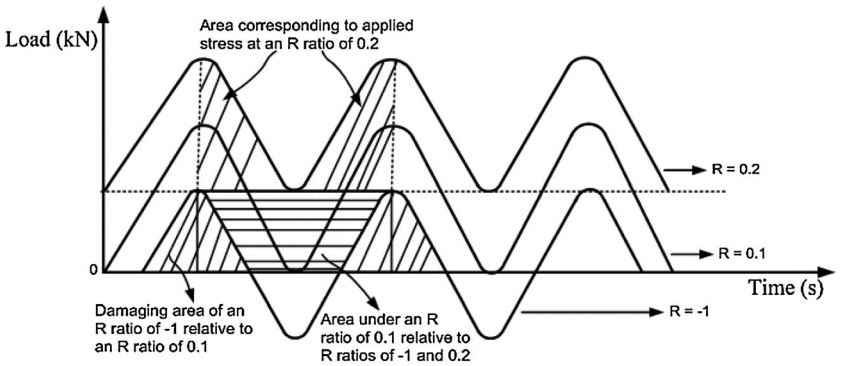

Fig. 3 Schematic diagram of area ratio correlation.

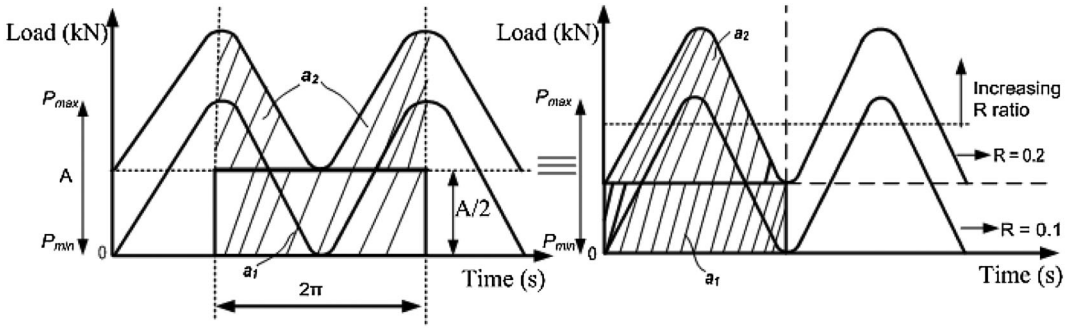

Fig. 4 Representation of crack opening area at positive R-ratios.

over a loading cycle, and the figure represents the R-ratios of 0.1 and 0.2 loading cycles. For other increasing R-ratios, the loading pattern will be similar to Fig. 2, and the area under an R-ratio of 0.1 will increase with respect to an increase in R-ratio. For the corresponding full corrosion effects at a positive R-ratio, the assumption made in the model development here is that only the tensile segment or the positive part of the loading cycle contributes to fatigue crack growth (tension–tension loading case). The crack opening at a positive R-ratio with reference to an R-ratio of 0.1 is highlighted by the shaded portion of Fig. 4. This implies that R-ratio effects on fatigue crack growth can be modelled using the crack growth response corresponding to an R-ratio of 0.1. The parameters in the figure are defined as follows:Area 1 (a_1) is the area of the rectangular segment of the shaded portion; Area 2 (a_2) is the area under the curve above a_1; $P_{\min}$ and $P_{\max}$ are the minimum and maximum applied loads in a cycle. It can also be seen that a_2 encompasses some portion of the sinusoidal curve in a_1, which is the area representing an R-ratio of 0.1 in the figure. This means that the damage cycle at a positive R-ratio of interest relative to that at an R-ratio of 0.1 with respect to the opening area situation can be given as

$$\frac{a_1 + a_2}{a_1}, \tag{12}$$

where for a loading cycle

$$a_1 = \pi A \tag{13}$$

$$a_2 = 2\left(\int_0^{P_{\max}} \int_0^{\pi} A sin\omega d\omega dA\right), \tag{14}$$

where A is amplitude, and ω is angular frequency. The dimensions of a_1 and a_2 are kN. Equation (12) is the area ratio theory multiplier for positive R-ratios in corrosion fatigue and is applied to modify the Paris law (Eq. (1)) as

$$\frac{da}{dN_{corr(+veR)}} = C_{corr}\left(\frac{a_1 + a_2}{a_1}\right)\Delta K^{m_{corr}\left(\frac{a_1+a_2}{a_1}\right)}, \tag{15}$$

where $\frac{da}{dN_{corr(+veR)}}$ is the crack growth rate for the positive R-ratio of interest, while C_{corr} and m_{corr} are the material constants corresponding to an R-ratio of 0.1. In order to obtain crack growth rates in air, Eq. (15) is applied by replacing C_{corr} and m_{corr} with C_{air} and m_{air}. However, it should be mentioned that the model developed in this paper and the corresponding Eqs (12) to (15) are only valid for sinusoidal waveforms.

Negative R-ratio

For an R-ratio of 0, $\Delta K = K_{\max}$, but for an R-ratio of −1, only the tensile or damaging portion of the loading cycle is effective in crack propagation. Hence, the compression portion of the loading cycle is neglected analytically on the premise that cracks close during compression. This means that the fatigue crack growth in this situation is controlled by $K_{\max}$ (the positive part of ΔK). This also implies that for a specific load/stress range, only half of the time of the fatigue cycle is spent in the damaging or crack opening situation at an R-ratio of −1. The model description is schematically shown in Figs. 5 and 6. If the two figures are superimposed for the crack opening period at R = –1 relative to R = 0.1, a_1 is equivalent to the area of the shaded portion under the sine curve for R = 0.1 (Fig. 5), while a_2 is the area of the (shaded) positive part of the sine curve for R < 0 (Fig. 6). The combination of Figs. 5 and 6 is shown in Fig. 7. Included in the figures are the corresponding tensile and compressive segments of the stress cycles. Therefore, the corrosion fatigue damage cycle at R = −1 relative to R = 0.1 for an opening area situation is defined as

$$\frac{a_2}{a_1} = \frac{2\left(\int_0^{P_{\max}} \int_0^{\pi} A sinwdwdA\right)}{\pi A} \tag{16}$$

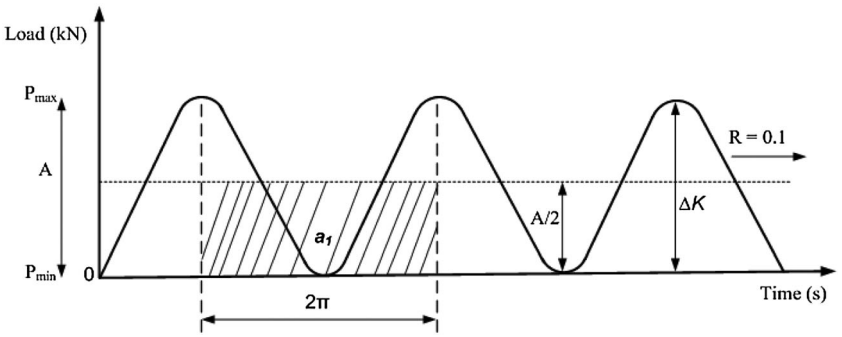

Fig. 5 Area of loading cycle corresponding to an R-ratio of 0.1.

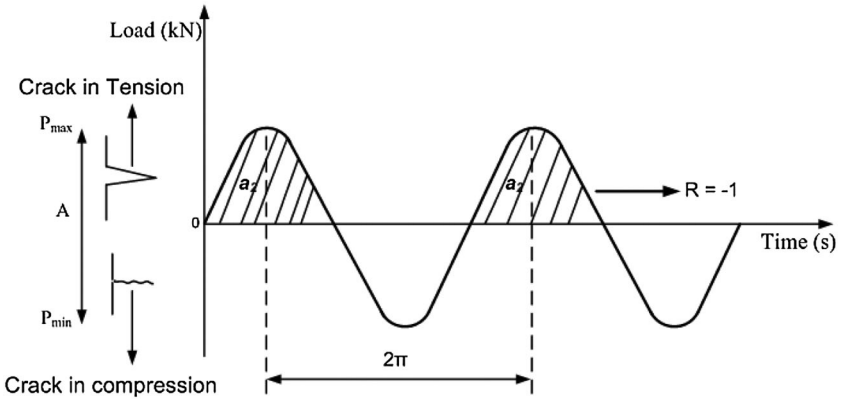

Fig. 6 Damaging portion of the loading cycle corresponding to an R-ratio of −1.

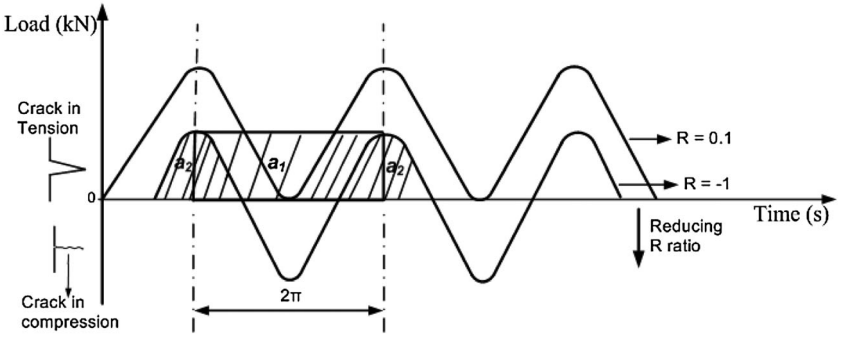

Fig. 7 Representation of crack opening area at negative R-ratios.

Equation (16) is the area ratio multiplier that is applied to predict corrosion damage at R = −1 with respect to the unified air and seawater crack growth response. The crack growth rates at R = −1 in seawater should lie between the air crack growth data and the crack growth rate obtained at the baseline full corrosion effect (R = 0.1). Also, considering only the positive part of the loading cycle, the stress intensity factor range ΔK in Eq. (1) is replaced by $K_{\max}$, and the crack growth rate in air is corrected as

$$\frac{da}{dN_{air\ R=-1}} = C_{air}(K_{\max})^{m_{air}} \tag{17}$$

Based on the methodology described previously combined with Eq. (17), the model for predicting crack growth rate in seawater at R = −1 is proposed as follows:

$$\frac{da}{dN_{corr(R=-1)}} = \left[C_{corr} + \frac{a_2}{a_1}(C_{air} - C_{corr})\right] K_{\max}{}^{\left(m_{corr}+\frac{a_2}{a_1}(m_{air}-m_{corr})\right)}, \tag{18}$$

where $\frac{da}{dN_{air\ R=-1}}$ and $\frac{da}{dN_{corr(R=-1)}}$ are the crack growth rates in air and seawater environments, respectively, at an R-ratio of −1, while C_{air} and m_{air} are material constants in air at an R-ratio of −1, and C_{corr} and m_{corr},

are material constants in seawater corresponding to an R-ratio of −1.

EXPERIMENTAL STUDIES

Fatigue crack growth tests were conducted in accordance with the ASTM E647 standard[30] on 16 mm thick compact tension specimens machined from S355J2 + N steel. The notches of the compact tension specimens were prepared by spark erosion and were positioned perpendicular to the rolling direction of the base plate. Constant amplitude sinusoidal loads were applied to the specimens using two 100 kN capacity servo–hydraulic fatigue machines at loading ratios of 0.1 and 0.5 and loading frequencies of 2 Hz in air and 0.3 Hz in artificial seawater. The artificial seawater was prepared in accordance with ASTM D1141[31] and was continuously circulated past the specimen at the rate of 3 L min^{-1}; the temperature was maintained at 8° to 10 °C.[6] Crack lengths were monitored by a digital camera, back face strain and direct current potential drop. Crack growth rates were determined from the plots of crack lengths versus the number of cycles using the seven point incremental polynomial method.

RESULTS AND DISCUSSION OF CORROSION FATIGUE CRACK GROWTH MODELLING

The predicted crack growth curves in seawater at positive R-ratios are shown, together with experimental data obtained at an R-ratio of 0.1, in Fig. 8 as plots of *da/dN* versus stress intensity factor range *K*. Stress ratio effects on fatigue crack growth were modelled at R-ratios of 0.2 to 0.7 relative to the baseline data (R-ratio of 0.1) using Eq. (15). It can be seen that the predicted crack growth curves move to the left of the baseline with increasing R and are parallel to each other with respect to the stress intensity factor ranges (ΔK). It was observed that the crack growth rates increased in a similar manner with respect to ΔK for all R-ratios. Crack growth rates were found to increase with an increase in R-ratio. At R-ratios of 0.1 to 0.4, similar *m* values were observed from the crack growth response, but the *C* values are different with respect to a particular R-ratio.

However, at the other higher stress ratios ($R \geq 0.5$), slightly higher slopes were obtained. The effect of higher mean stress can be seen in Fig. 8 by the noticeable deviations between the crack growth curves at higher R-ratios compared with the lower values. This implies that at higher stress ratios, the crack faces are fully open. Therefore, a crack closure free condition occurs, such that the crack face does not come in contact during the unloading portion of the stress cycle. Another explanation of this is that at a higher stress ratio in seawater, the magnitude of the corrosive elements entering the crack tip are relatively greater than at a lower stress ratio because of the mechanisms of crack tip opening displacement or opening area and the associated stress levels in promoting rapid crack growth. As such, this synergistic interaction between the applied high-stress ratio and the corrosive environment are therefore expected to enhance the corrosive activity in the crack tip.

Model validation at positive R-ratios in seawater

The validation of the present model is demonstrated in Fig. 9. The figure compares experimental data obtained at R-ratios of 0.1 and 0.5 in seawater with modelled crack

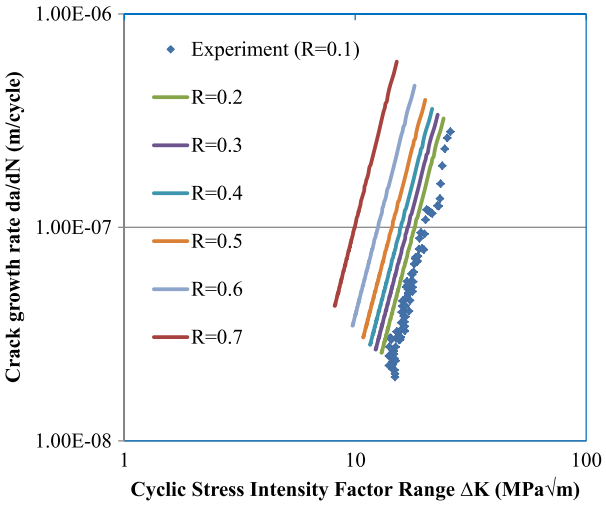

Fig. 8 Predicted crack growth rates at positive R-ratios.

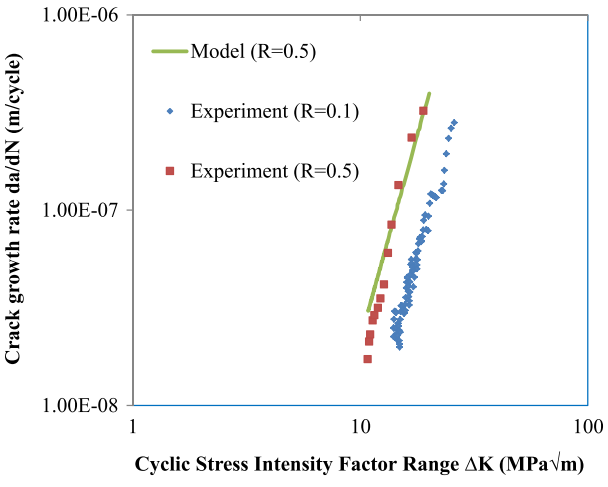

Fig. 9 Comparison of predicted crack growth rates with experimental data in seawater.

growth curves at an R-ratio of 0.5. Experimental data obtained at other higher R under similar test conditions are lacking and are therefore not considered in the comparison. However, the present model can be utilised to predict crack growth rates at a particular R-ratio when experimental data for such loading conditions are not available provided the R-ratio of interest is within the range of validity of the present model. It can be seen from Fig. 9 that the predicted crack growth curve using Eq. (15) gave a fairly good agreement with the experimental data, as shown by the similarity in crack growth trends.

The predictions of Eq. (15) are compared with the observed crack growth rates in seawater at an R-ratio of 0.1, as shown in Fig. 10. It was observed that nearly 70% of the data points were within ±20% with a mean percentage absolute error of 0.18. The data points that fell outside ±20% are those that were obtained particularly at lower ΔK. This may be as a result of the significant number of data points recorded during testing. It should be mentioned that the comparison made for an R-ratio of 0.1 was based on back substitution of the C and m values into the crack growth model. However, this would be useful for discussion for the comparison made at an R-ratio of 0.5.

The predicted crack growth rates using Eq. (15) are compared with those measured experimentally at an R-ratio of 0.5 in seawater, as shown in Fig. 11. With reference to the crack growth data plotted in Fig. 9, it can be observed that the modelled crack growth curve at an R-ratio of 0.5 was obtained from a significant number of experimental baseline data compared to those obtained at an R-ratio of 0.5 experimentally. Therefore, the data plotted in Fig. 11 are the corresponding experimental and modelled crack growth rates obtained at an R-ratio of 0.5 with similar values of ΔK. This was the only

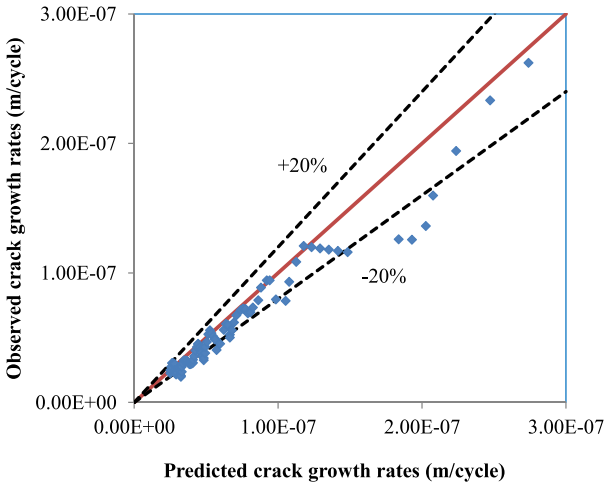

Fig. 10 Observed versus predicted crack growth rates in seawater at an R-ratio of 0.1.

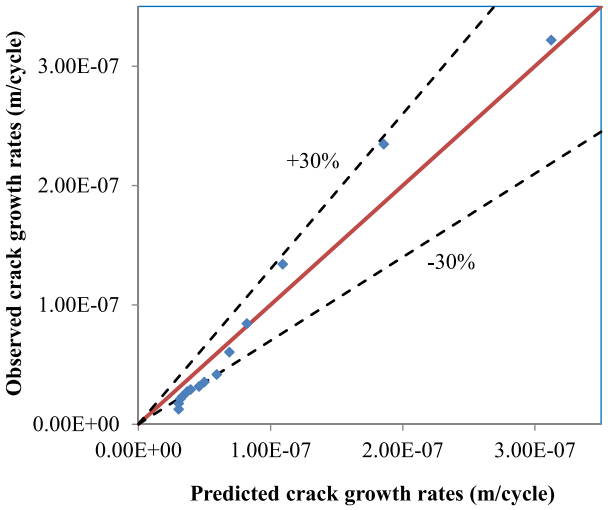

Fig. 11 Observed versus predicted crack growth rates in seawater at an R-ratio of 0.5.

alternative for the comparisons made in the figure. However, the crack growth trends are nearly the same, regardless of the number of experimental data points, as shown in Fig. 9. It was also observed, as shown in Fig. 11, that there was a fairly good correlation with the experimental data and also the majority of the data points are predicted to be within ±30% with a mean percentage absolute error of approximately 0.3. Therefore, it can be implied that the present model is, to a reasonable degree, good for predicting crack growth data for positive R-ratios.

The model developed for the positive R-ratio case was compared with the seawater baseline data and with data corresponding to the R-ratios of 0.1 in 2,3,10,32 as shown in Fig. 12. It can be seen that the present model agrees well with the experimental data. There is also a reasonable agreement between the present experimental data and those obtained by Appleton[10] and Thorpe *et al.*[2], particularly at lower ΔK, but at higher ΔK, the present model and experimental data fall between the data of Appleton and Thorpe *et al.*, respectively. The environmental test conditions of the results plotted in Fig. 12 are different from each other with respect to the composition of the seawater, and it is anticipated that the effect of the corrosive environment will be dominant at higher ΔK. Therefore, the crack growth trends in the figure at higher ΔK may be expected. It can also be seen that the present data increased in a monotonic manner over the entire ΔK while the crack growth trends of Appleton's study are not consistent and converged with the data of Thorpe *et al.* at higher ΔK. Coupled with a difference in cyclic load frequency, it is also possible that the difference in chemical composition and mechanical properties of the C-Mn steel used by Appleton was related to the crack growth trend observed in Fig. 12. It is expected that crack growth rates would increase with an

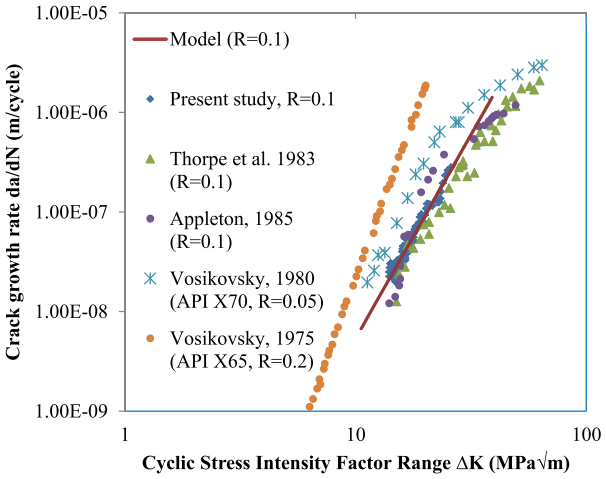

Fig. 12 Model comparison with experimental data at an R-ratio of 0.1 and 0.2 in seawater.

increase in R-ratio, as demonstrated by the present study and as reported by Thorpe *et al.*, despite the amount of scatter in their results, but no effect of R-ratio was seen in Appleton's study at either free corrosion potential or under cathodic protection. Details of this can be found in 10. The implication of this is that mean stress effects on crack growth rates are material dependent. Included in Fig. 12 are data obtained from API X65 and API X70[3,32] at R-ratios of 0.05 and 0.2, respectively. It can be seen that the API X65 steel crack growth data shifted to the left of the model as expected. This could be attributed to the difference in stress ratio and material.

The model was further compared with experimental data collected at an R-ratio of 0.5 from 2 and 10, as shown in Fig. 13. Included in the figure are the same experimental data plotted in Fig. 9. It can be observed from the figure that the present experimental data appear better when compared with both Appleton's data[10] and the significant scatter observed in the data of Thorpe *et al.*[2] The predicted curve yields a fairly good agreement with the experimental data, and it can also be seen that the data of Thorpe *et al.* agrees fairly well with those realised in this study. However, it is worth mentioning that the effects of cathodic protection, applied load and load frequency used in the investigations of Thorpe *et al.* and temperatures used for testing in Appleton's study could have a significant effect on the crack growth rates compared with the present study. Therefore, it is important to understand the interaction of these parameters and most importantly the frequency content of the stress cycle for fatigue assessment and results comparison.

Figure 14 compares the present model with data obtained using the ASTM artificial seawater at various temperatures.[10] It can be seen that there is little effect of temperature on crack growth rates. It is possible that the varying amount of dissolved oxygen was responsible for this effect but this was not considered in the present study. It can also be seen that the present model overestimated Appleton's data and shifted to the left of the data points. This could be attributed to the effect of applied load range. From the data analysis, the minimum ΔK in the R-ratio of 0.5 test was 10 MPa $\sqrt{m}$, while in Appleton's study for the three cases plotted in Fig. 14, the minimum ΔK was in the range of 13 to nearly 16 MPa $\sqrt{m}$, which indicates an effect of the applied load. Therefore, such a shift in the present modelled curve relative to experimental data, as shown in Fig. 14, should be expected. It can also be seen that the crack growth trends of the three cases plotted in the figure are quite similar to the modelled curve between the ΔK

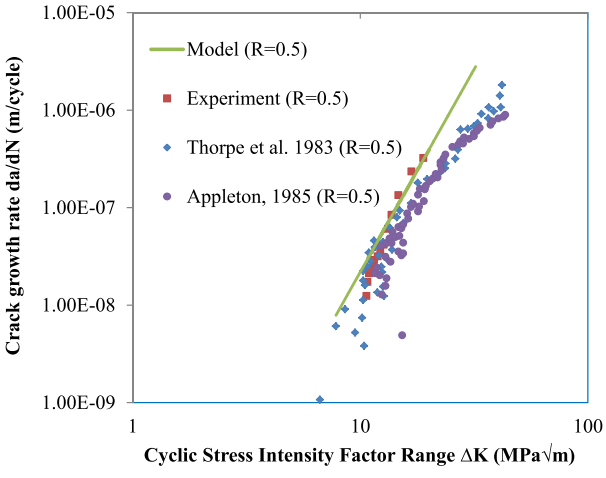

Fig. 13 Model comparison with experimental data at an R-ratio of 0.5 in seawater.

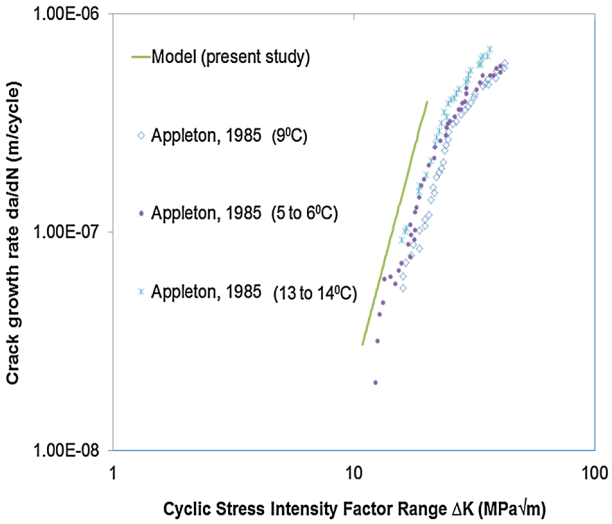

Fig. 14 Model comparison with Appleton's data at an R-ratio of 0.5.

ranges of 10 to 20 MPa $\sqrt{m}$, above which the crack growth trends deviate towards the right, resulting in a bi-linear relationship. This may be due to differences in specimen geometry and loading type.

The predicted crack growth curves using Eq. (15), coupled with the material parameters derived at R-ratios of 0.1 and 0.5, are shown in Fig. 15 as comparisons with the experimental data. The modelled curves showed similar crack growth trends to the experimental data across the range of loading cycles. However, towards the end of the test duration, a marginal difference in the number of loading cycles was observed in the R = 0.1 test, which may be due to experimental uncertainties. In the R = 0.5 test, a higher crack growth was measured compared to the predicted one, as shown in Fig. 15. However, in this situation, the prediction can be considered conservative for estimating fatigue lives of offshore installations. It should be noted that these are not entirely independent predictions, particularly at an R-ratio of 0.1 as the C and m values from the same tests were back substituted into the crack growth model.

This approach can also be extended to predict the lifetime of a welded joint considering a near-surface residual stress distribution because it may be assumed that the life of a welded joint is consumed under a high-stress ratio, as mentioned previously, because of the significant levels of weld-induced residual stresses present. However, for a through-thickness residual stress distribution that is found in relatively thick welded steel materials with a similar thickness to that used in newer types of offshore structures, the magnitude of the residual stress distribution may be compressive compared with the near-surface tensile residual stress. Therefore, Eq. (15) cannot accurately predict crack growth rates, and Eq. (18) can be recommended for predictions in such situations.

Model validation at a positive R-ratio in air

The predictions of Eq. (15) are compared with the experimental data obtained at the R-ratios of 0.1 and 0.5 in air, as shown in Fig. 16. It can be observed that the two predicted curves are parallel to each other resulting in similar m values but different C values as expected. The predicted crack growth rates agree well with the experimental data, particularly at an R-ratio of 0.1. However, at an R-ratio of 0.5, the predicted crack growth curve deviated from the experimental data, particularly at lower ΔK, but at higher ΔK, the predicted curve agrees fairly well with the experimental data. The observed difference between the predicted and measured crack growth rates might be due to the response of the material to mean stress effects at lower ΔK with respect to the material properties. However, observations revealed that the differences in the modelled result and the air data comparison (Fig. 16) are small and within experimental scatter.

Also, the trend of the air and seawater data (Figs. 9 and 16) implies that crack growth rate is more sensitive to mean stress effects at higher ΔK ranges than at lower ones. The model comparison with experimental results appears better in seawater (Fig. 9) than in air. This is probably due to the fact that at a particular stress ratio, the synergistic effects of the corrosive environment and cyclic frequency would enhance the fatigue damage process. Therefore, dissimilar crack growth behaviour may be expected in the air environment where the crack driving force ΔK and crack growth rates were only influenced by the applied stress ratio. This suggests that the influence of the R-ratio on crack growth rates is significantly higher in seawater than in air. The predicted crack growth rates in air at an R-ratio of 0.1 using Eq. (15) are compared with the experimental ones, as shown in

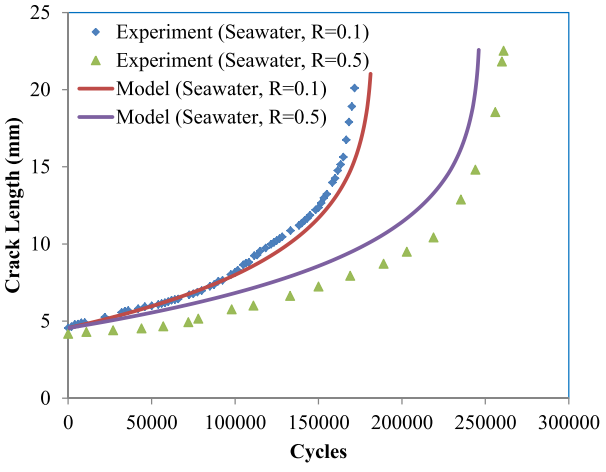

Fig. 15 Comparison of predicted crack growth in seawater with experimental data at R-ratios of 0.1 and 0.5.

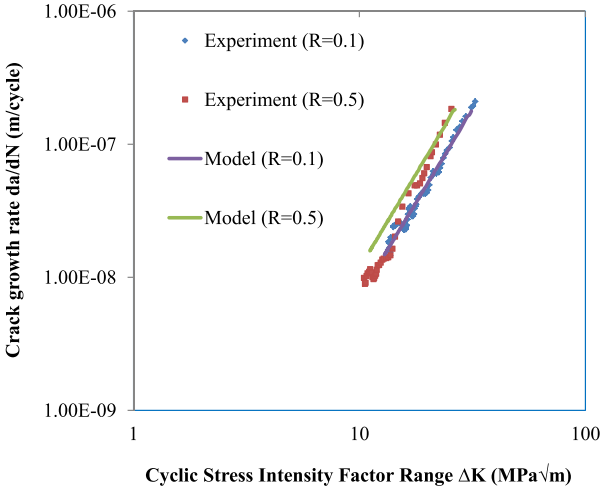

Fig. 16 Comparison of the predicted crack growth rates in air with experimental data.

Fig. 17. The data points are predicted to within ±20%. It was found that nearly 90% of the data points were within ±20% with a mean absolute percentage error of 0.11, which indicates a fairly good prediction.

In Fig. 18, the measured crack growth rates in air at an R-ratio of 0.5 are compared with those predicted using Eq. (15). The data points were predicted to within ±30% with a mean absolute percentage error of 0.4. The calculated mean absolute percentage error and the corresponding number of data points that fell outside ±30% in the parity plots, as shown in Fig. 18, also suggest that the new correlation represents the experimental data fairly well. Figure 19 compares the predicted crack growth curves in air with experimental data. The modelled curves advanced in a similar manner to the experimental results over the entire test duration, as shown in the figure, but the model slightly overpredicted the experimental data; however, this difference can be regarded as marginal considering the similarity in the shape of the curves.

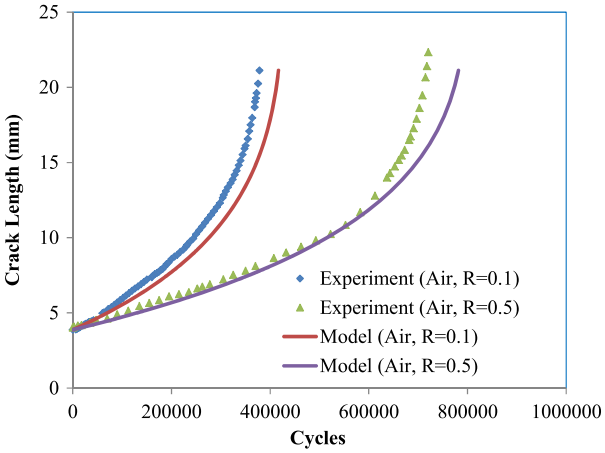

Fig. 19 Comparison of predicted crack growth in air with experimental data at R-ratios of 0.1 and 0.5.

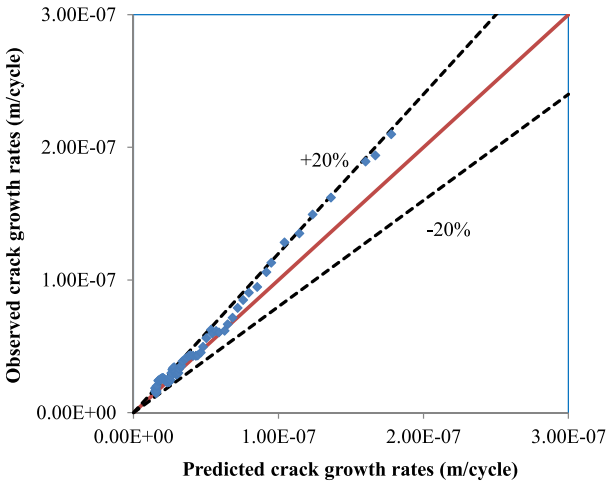

Fig. 17 Observed versus predicted crack growth rates in air at an R-ratio of 0.1.

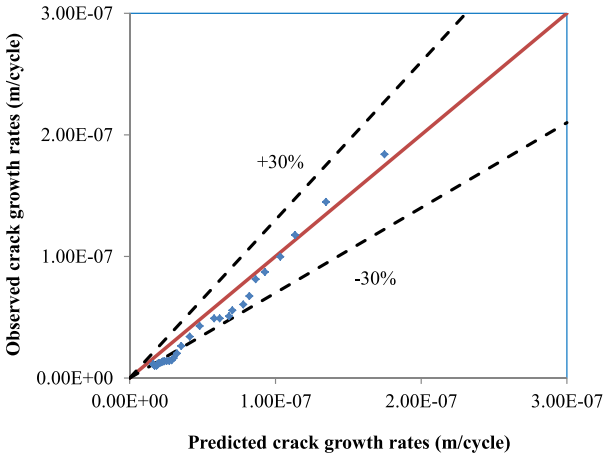

Fig. 18 Observed versus predicted crack growth rates in air at an R-ratio of 0.5.

Further comparisons are made between the predicted and experimental lives in air and in seawater, as shown in Table 1. The ratios of the predicted to the measured life range from 0.94 to 1.01. Correlations of predictions with experimental data have been considered as accurate if the ratio of the predicted to the experimental life is 1.[33] The ratios depicted in Table 1 are nearly 1, which implies that the present model might therefore be considered suitable for fatigue life calculations following more validation against experimental tests.

Discussion of negative R-ratio data

For the negative R-ratio case, the crack growth rates obtained at an R-ratio of 0.1 in air were corrected by replacing ΔK by K_{max} in Eq. (1) to obtain Eq. (17) in terms of the dominant crack driving parameter (K_{max}). This implies that only the tensile segment of the stress cycle is considered to be the effective region responsible for crack growth. This result is plotted in Fig. 20, and

Table 1 Comparison of experimental and predicted lives in air and seawater

Stress Ratio (R)	Experimental life, N_{exp} (Cycles)	Predicted life, N_{pred} (Cycles)	N_{pred}/N_{exp}
Air			
0.1	378 500	417 000	1.10
0.5	720 500	781 600	1.08
Seawater			
0.1	171 650	181 200	1.05
0.5	261 000	246 000	0.94

included in the figure are the experimental data obtained at an R-ratio of 0.1. As mentioned earlier, it is assumed that the predicted crack growth rates at an R-ratio of −1 in seawater would lie between the air and seawater data obtained at an R-ratio of 0.1. The derived crack growth data in air using Eq (17) was utilised to achieve this procedure. The result is shown in Fig. 20 where it can be seen that the crack growth curve for an R-ratio of −1 shifted to the right of the baseline data (R = 0.1). Crack growth rates were also found to be higher at an R-ratio of 0.1 than at an R-ratio of −1 as expected.

Figure 21 also shows a comparison between the prediction of Eq. (17) and the experimental result obtained at an R-ratio of 0.1 as a plot of crack length versus number of cycles. A noticeable difference of approximately one third of the number of cycles consumed at an R-ratio of 0.1 was observed between the two curves. Figure 22 shows the predictions of fatigue crack growth in seawater for a negative R-ratio using Eq. (18). The predicted curve is compared with experimental data obtained in air and in seawater at an R-ratio of 0.1 for both. It can be seen that the predicted curve lies between the seawater and the air data and moves to the right of the seawater curve, which implies the mean stress effect at R-ratio of −1 is clearly demonstrated. Crack growth rates were also shown to be higher at an R-ratio of 0.1 than at an R-ratio of −1. This appears practical because only half of the stress cycle was spent in the damaging portion at an R-ratio of −1 compared with the wholly tensile loading of an R-ratio of 0.1.

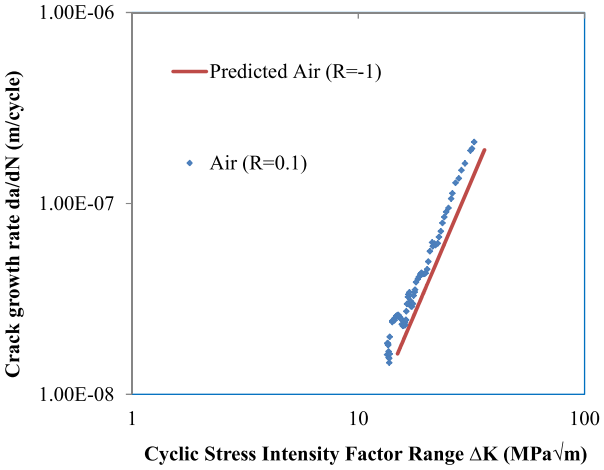

Fig. 20 Crack growth rates in air.

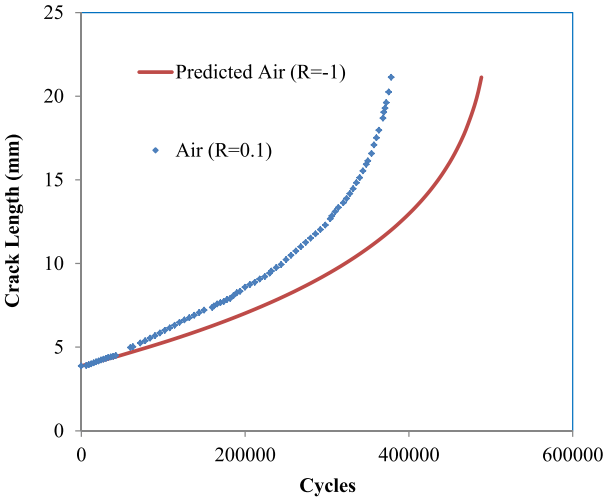

Fig. 21 Fatigue crack growth in air.

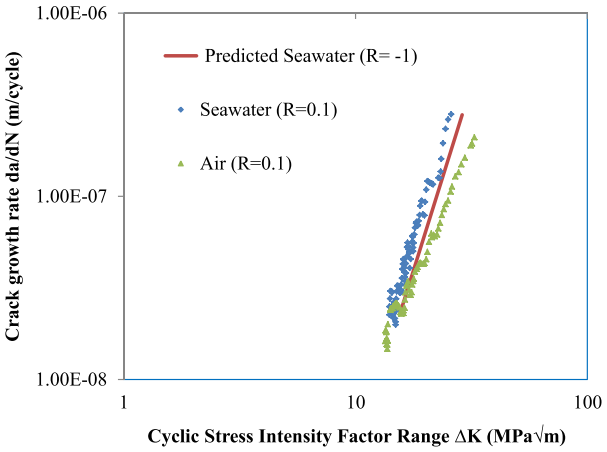

Fig. 22 Comparison of the predicted crack growth rates in seawater with experimental data.

Therefore, it is expected that the degree of damage caused in the R-ratio of 0.1 test will be relatively higher than at an R-ratio of −1 where the crack propagation with respect to environmental damage would be limited to the tensile segment or half the stress cycle. The significance of the model (Eq. (18)) for negative R-ratios is its ability to predict the material behaviour under the action of tension–compression loading in seawater using the material response data obtained in air and seawater under tension – the tension loading case. The novel modelling procedure developed and discussed in this section may be adequate for generating data for a positive and negative R-ratio without testing.

Model comparison with other fatigue crack propagation models

The present model was also verified by comparing the response with some of the previously described fracture mechanics-based models given in Eqs (5) to (11). Crack growth curves in air are compared in Fig. 23. In Fig. 23a, the present model and all the other applied models are parallel with the experimental data obtained at an R-ratio

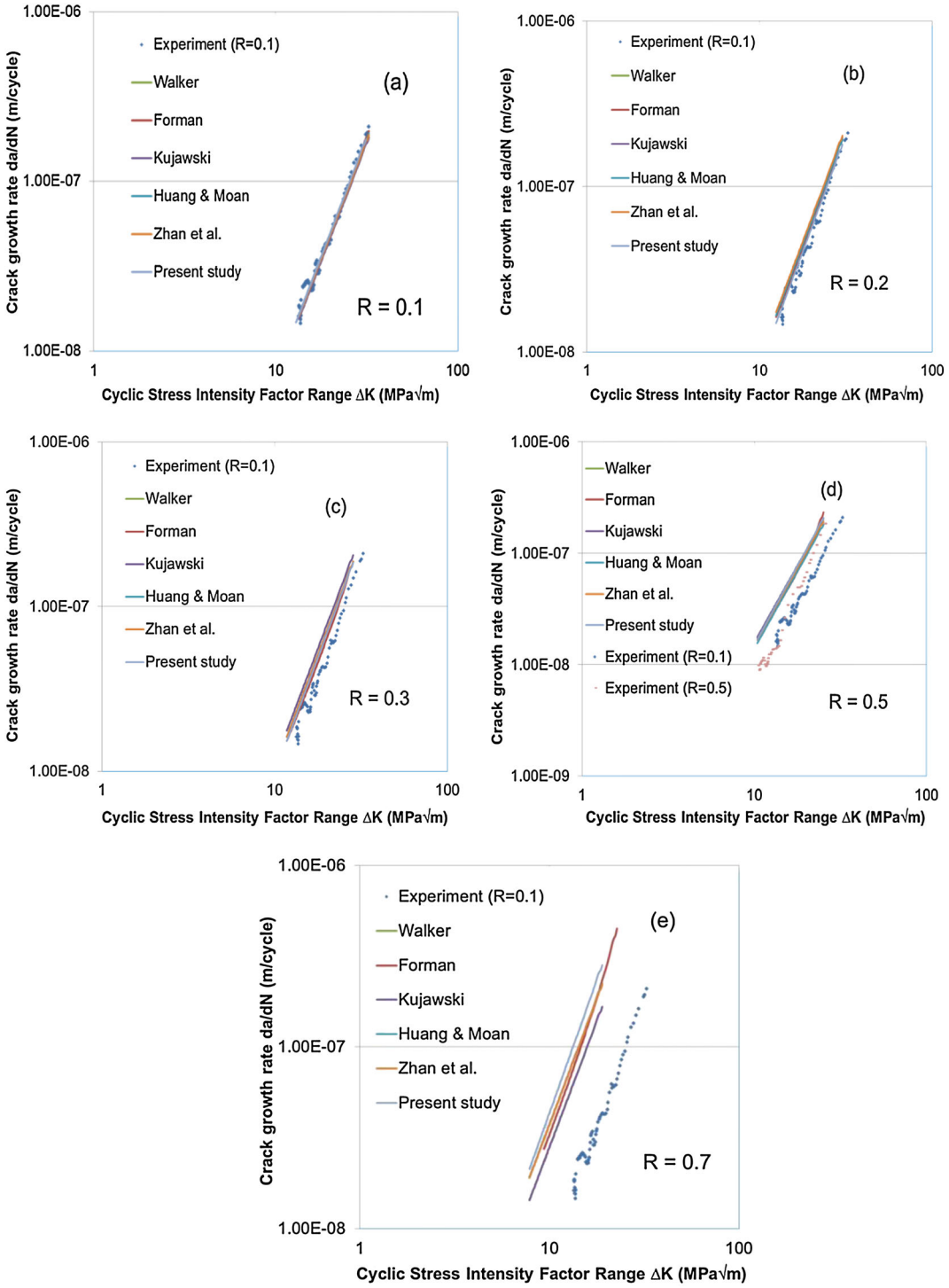

Fig. 23 Model comparison with other crack propagation models in air.

of 0.1 in air. As the R-ratio was increased (Fig. 23b–e), the predicted curves shifted to the left of the baseline as expected.

The present model agrees well with the other models examined in air from R-ratios of 0.1 to 0.5, as shown in Fig. 23. At an R-ratio of 0.7, Kujawski's and Walker's predicted curves are parallel and resulted in lower growth rates compared with the present model and the predictions of Zhan *et al.* It can also be observed from Fig. 23e that the Zhan *et al.* and Forman predicted curves are

closer to the present model compared with the remaining models tested and with the Forman predicted curve deviating at a higher ΔK. The inconsistent responses from the models, particularly at an R-ratio of 0.7, may be due to the difference in correction factors associated with the models, which is likely to have appreciable effects on crack growth rates at higher stress ratios because of the associated stress levels.

The predicted crack growth curves in seawater are compared in Fig. 24, and it can be seen that the present

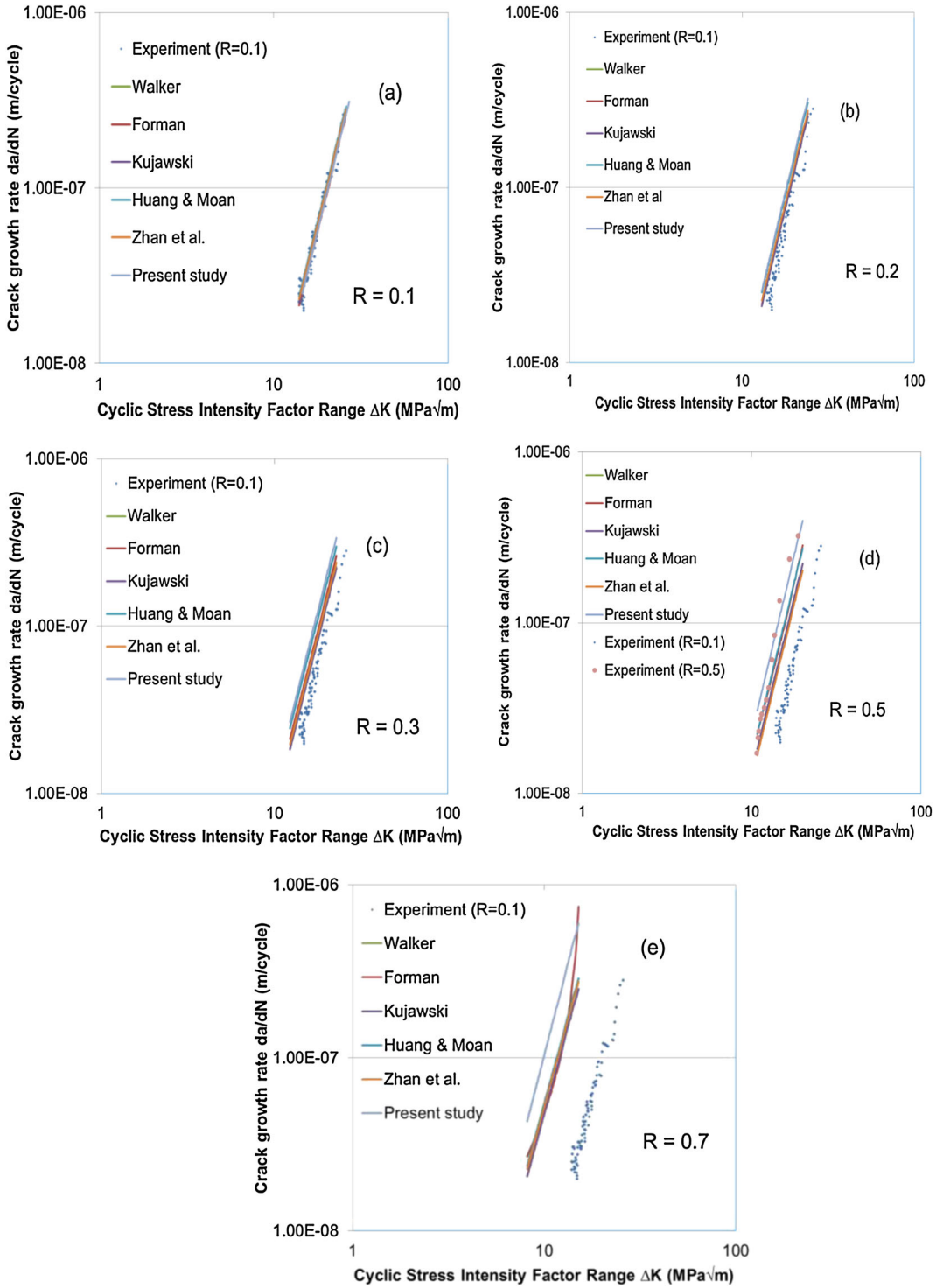

Fig. 24 Model comparison with other crack propagation models in seawater.

model agrees well with the other models at R-ratios of 0.1 and 0.2. These results are shown in Fig. 24a and b. At an R-ratio of 0.3, only Huang and Moan's model agrees with the proposed model, while Kujawski's and Walker's predicted curves deviate from the other predictions. At an R-ratio of 0.5 and 0.7, the present model somewhat overestimated the crack growth rates compared with the other models and converged with the Forman predicted curve at a higher ΔK. It should be noted that the crack propagation mechanism in seawater is different from that in air due to the various factors contributing to the process. Therefore it is expected that the mean stress effect will be more significant in seawater than in air. Comparing the general behaviour of the models used for prediction against the current model, much better agreement was observed at all the positive R-ratios considered in air and at lower R-ratios in a seawater environment. The present model agrees fairly well for the cases considered in the present investigation.

To verify the accuracy of the present model for the negative R-ratio case in seawater, the predicted curve using Eq. (18) is compared with the other examined models, as shown in Fig. 25. The comparison was made considering only the models that are valid for a negative R-ratio, as previously described. The model yields a good agreement with the other tested models as shown in the figure. This is evident from the similarity in the curves over all the range of loading cycles. From the results and analysis carried out in this paper, it should be mentioned that the present model appears better for negative R-ratio cases than the positive cases in air and seawater, respectively. Lower or higher mean stresses can be introduced in offshore structures from welding, deflection and bending moments because of lateral loads continuously acting on the structures in service. Therefore, the analyses made in this paper may represent both tensile and compressive mean stress/residual stresses, depending on their locations within the structure.

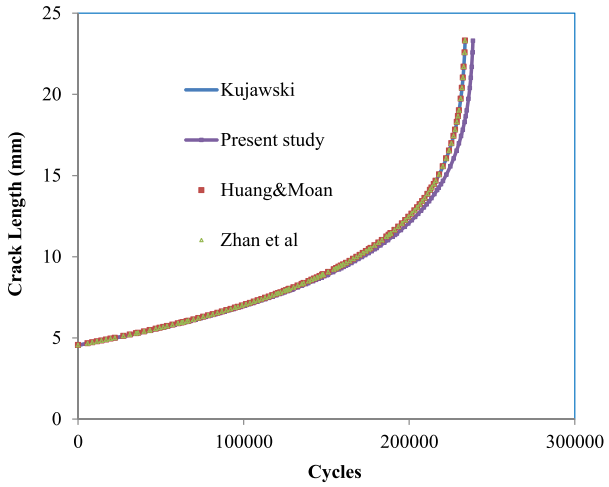

Fig. 25 Comparison of predicted fatigue crack growth in seawater at R-ratio of −1.

CONCLUSIONS

Fatigue crack growth experimental tests were conducted on S355J2 + N steel in air and in a free corrosion seawater environment. A model was developed to account for mean stress effects on fatigue crack growth in air and seawater. The methodology used for the model development is unique and not considered by the current fracture mechanics-based models. The following tentative conclusions can be drawn from the study with the caveat that further testing for validation is required:

(1) Crack growth rates were higher in seawater than in air across all the stress intensity factor ranges tested.
(2) The proposed model is limited to stage II of fatigue crack growth (Linear Elastic Fracture Mechanics), and its applicability is valid for stress ratio in the range of −1 to 0.9.
(3) Because of the time and cost involved in conducting experimental tests at all the possible stress ratios, modelling the R-ratio effects on crack growth rates may be a valid and cost effective approach for generating data for fatigue life calculations.
(4) The new model gave a fairly good agreement when compared with experimental data obtained in air and free corrosion conditions.
(5) The overall comparison of the present model with other fracture mechanics-based models that account for mean stress effects on fatigue crack growth yields a fairly good result.
(6) A comparison of the present model appears better for negative R-ratio than the positive ones.

Acknowledgements

The authors acknowledge the support of the Petroleum Technology Development Fund, Nigeria, which is supporting the PhD of O. Adedipe.

REFERENCES

1 Brennan, F. P. (2014) A framework for variable amplitude corrosion fatigue materials tests for offshore wind steel support structures. *Fatigue Fract. Eng. Mater. Struct.*, **37**, 1–5.
2 Thorpe, T. W., Scott, P. M., Rance, A. and Silvester, D. (1983) Corrosion fatigue of BS 4360:50D structural steel in seawater. *Int. J. Fatigue*, **5**, 123–133.

3 Vosikovsky, O. (1975) Fatigue crack growth in an X-65 pipeline steel at low cyclic frequencies in aqueous environments. *Trans. ASME, J. Eng. Mater. Technol.*, **97**, 298–304.
4 Barsom, J. M. (1971) Corrosion-fatigue crack propagation below KISCC. *Eng. Fract. Mech.*, **3**, 15–25.
5 Gingell, A. D. B. and King, J. E. (1997) The effect of frequency and microstructure on corrosion fatigue crack propagation in high strength aluminium alloys. *Acta Mater.*, **45**, 3855–3870.
6 Adedipe, O., Brennan, F. and Kolios, A. (2015) Corrosion fatigue load frequency sensitivity analysis. *Mar. Struct.*, **42**, 115–136.
7 Havn, T. and Osvoll, H. (2002) Corrosion fatigue of steel in seawater. In: *NACE International Corrosion Conference*, no. 02431, 1–11.
8 Yu, J., Brook, R., Cole, I., Morabito, D. and Demofonti, G. (1996) The effect of cathodic protection potential on corrosion fatigue crack growth rate of an offshore structural steel. *Fatigue Fract. Eng. Mater. Struct.*, **19**, 1019–1029.
9 Kermani, M. B. and Harrop, D. (1996) The impact of corrosion on oil and gas industry. *Soc. Pet. Eng.*, **11**, 186–190.
10 Appleton, R. J. (1985) Corrosion fatigue of a C-Mn steel. PhD Thesis, University of Glasgow.
11 Barsom, J. M. (1972) Effect of cyclic stress form on corrosion fatigue crack propagation below KISCC in a high yield strength steel. In: *Corrosion Fatigue: Chemistry, Mechanics and Microstructure* (Edited by O. F. Devereux, A. J. McEvily and R. W. Staehle), Vol. NACE-2, National Association of Corrosion Engineers, Houston, pp. 424–436.
12 McClung, R. C. (2007) A literature survey on the stability and significance of residual stresses during fatigue. *Fatigue Fract. Eng. Mater. Struct.*, **30**, 173–205.
13 Antunes, F. V., Chegini, A. G., Camas, D. and Correia, L. (2015) Empirical model for plasticity-induced crack closure based on Kmax and ΔK. *Fatigue Fract. Eng. Mater. Struct.*, **38**, 983–996.
14 Paris, P. C. and Erdogan, F. (1963) A critical analysis of crack propagation laws. *J. Basic Eng.*, **85**, 528–534.
15 Zhan, W., Lu, N. and Zhang, C. (2014) A new approximate model for the R-ratio effect on fatigue crack growth rate. *Eng. Fract. Mech.*, **119**, 85–96.
16 Elber, W. (1971) The significance of fatigue crack closure. In: *Damage tolerance in aircraft structures*, American Society for Testing and Materials (ASTM) STP 486: Philadelphia, 230–242.
17 Maddox, S. J., Gurney, T. R., Mummery, A. M. and Booth, G. S. (1978) An investigation of the influence of applied stress ratio on fatigue crack propagation in structural steels. *Welding Institute Research Report*, 72/1978/E.
18 Schijve, J. (1981) Some formulas for the crack opening stress level. *Eng. Fract. Mech.*, **14**, 461–465.
19 Kumar, R. and Singh, K. (1995) Influence of stress ratio on fatigue crack growth in mild steel. *Eng. Fract. Mech.*, **50**, 377–384.
20 Lin, H.-C. and Kujawski, D. (2008) A general equation for Kop and KPR description. *Eng. Fract. Mech.*, **75**, 3244–3248.
21 Chen, D. L., Weiss, B. and Stickler, R. (1996) Contribution of the cyclic loading portion below the opening load to fatigue crack growth. *Mater. Sci. Eng.*, **208**, 181–187.
22 Donald, K. and Paris, P. C. (1999) An evaluation of Keff estimation procedures on 6061-T6 and 2024-T3 aluminium alloys. *Int. J. Fatigue*, **21**, 47–57.
23 Kujawski, D. (2001) Enhanced model of partial crack closure for correlation of R-ratio effects in aluminum alloys. *Int. J. Fatigue*, **23**, 95–102.
24 Walker, K. (1970) The effect of stress ratio during crack propagation and fatigue for 2024-T3 and 7076-T6 aluminium. In: *Effect of environment and complex load history on fatigue life*, American Society for Testing and Materials (ASTM) STP 462: Philadelphia, 1–14.
25 Kujawski, D. (2001) A new driving force parameter for crack growth in aluminum alloys. *Int. J. Fatigue*, **23**, 733–740.
26 Kujawski, D. (2001) A fatigue crack driving force parameter with load ratio effects. *Int. J. Fatigue*, **23**, 239–246.
27 Dinda, S. and Kujawski, D. (2004) Correlation and prediction of fatigue crack growth for different R-ratios using Kmax and ΔK+ parameters. *Eng. Fract. Mech.*, **71**, 1779–1790.
28 Noroozi, A. H., Glinka, G. and Lambert, S. (2007) A study of the stress ratio effects on fatigue crack growth using the unified two-parameter fatigue crack growth driving force. *Int. J. Fatigue*, **29**, 1616–1633.
29 Huang, X. and Moan, T. (2007) Improved modeling of the effect of R-ratio on crack growth rate. *Int. J. Fatigue*, **29**, 591–602.
30 ASTM E647 (2008) Standard test method for measurement of fatigue crack growth rates.
31 ASTM D1141 (2008) Standard practice for the preparation of substitute ocean water.
32 Vosikovsky, O. (1980) Effects of stress ratio on fatigue crack growth rates in X70 pipeline steel in air and saltwater. *J. Test. Eval.*, **8**, 68–73.
33 Beden, S. M., Abdullah, S. and Ariffin, A. K. (2009) Review of fatigue crack propagation models for metallic components. *Eur. J. Sci. Res.*, **28**, 364–397.